Uniform Global Exponential Stabilizing Passivity-Based Tracking Controller Applied to Planar Biped Robots

Pierluigi Arpenti[1], Alejandro Donaire[2], Fabio Ruggiero[1], and Vincenzo Lippiello[1]

***Abstract*— This paper presents a novel control approach, based on the interconnection and damping-assignment passivity-based control (IDA-PBC), to achieve stable and periodic walking for underactuated planar biped robots with one degree of underactuation. The system's physical structure is preserved by assigning a target port-Hamiltonian dynamics to the closed-loop system, which also ensures passivity. The control design ensures that the tracking error to the desired periodic gait converges exponentially to zero, and the convergence rate can be adjusted via gain tuning. Besides, through the hybrid zero dynamics, the stability of the full-order system can be retrieved from the stability of the orbit created in a lower-dimensional manifold. The proposed approach is the first example of a tracking controller based on the IDA-PBC applied to underactuated biped robots. Numerical simulations on a five-link planar biped robot with unactuated ankles validate the approach and show the performance of the closed-loop system.**

I. Introduction

Bipedal locomotion is characterized by continuous swing phases, in which only one foot is in contact with the ground, alternated by discrete impact events occurring at foot landing. The stance foot rotates around the contact point with the ground during each continuous phase, with zero control torque. Therefore, biped robots emulating human walking are underactuated and hybrid [1].

Hybrid zero dynamics (HZD) is a fundamental control design tool for biped robots [2]. This approach creates a stable periodic orbit in a lower-dimensional manifold by zeroing some output variables defined in terms of *virtual constraints* imposed via feedback. The HZD evolves on such a lower-dimensional space and constitutes an extension of the concept of zero dynamics [3] to hybrid systems. The lower-dimensional manifold is *hybrid invariant*, that is, invariant under both the robot's continuous and discrete dynamics. For planar bipeds walking along their sagittal plane only, hybrid invariance arises from the exponential convergence of the output variables, referred to as *transverse dynamics*, to the HZD manifold [4]. The motivation is the repulsive behaviour of the impact map, which rejects the transverse solutions far away from the HZD manifold. Hence, an exponentially fast convergence rate is required to counteract the reset map.

The research leading to these results has been supported by the PRINBOT project, in the frame of the PRIN 2017 research program (grant no. 20172HHNK5_002), and the COWBOT project, in the frame of the PRIN 2020 research program (grant no. 2020NH7EAZ_002).

[1] PRISMA Lab, Department of Electrical Engineering and Information Technologies, University of Naples Federico II, Via Claudio 21, Naples, Italy. Corresponding author's e-mail: pierluigi.arpenti@unina.it.

[2] The University of Newcastle, University Drive, Callaghan, 2308, NSW, Australia.

Control strategies exploiting the HZD concept were initially based on the input-output linearization (IOL) of the biped's nonlinear (natural) transverse dynamics followed by a proportional-derivative (PD) control to impose an exponential convergence to the HZD manifold. Successively, an approach based on control Lyapunov functions (CLF), namely the rapidly exponentially stabilizing control Lyapunov function (RES-CLF), was presented to go beyond simple PD controller while guaranteeing a sufficiently fast exponential converge of transverse dynamics [5]. Methodologies based on IOL require the total cancellation of natural dynamics. Consequently, the closed-loop robustness to parametric uncertainties is endangered. Recently, a passivity-based controller was presented to preserve the nonlinear dynamics of the system [6]. Such a method performs only partial cancellations of the nonlinear dynamics, yielding a closed-loop system that is more robust.

All the methodologies proposed so far are rooted in the *Lagrangian* modelling formalism. An alternative is the *port-Hamiltonian* (pH) framework [7], which describes systems in terms of the interconnection between energy-conserving and energy-dissipating structures. One of the control strategies proposed in the pH formalism is the *interconnection and damping assignment passivity-based control* (IDA-PBC) [8] which has mainly been adopted in the stabilization of underactuated mechanical systems [9]. This methodology reshapes the system's physical properties by assigning a target closed-loop pH system with desired characteristics, preserving passivity. Recently, alternative versions of IDA-PBC were used to generate new gaits for an underactuated compass-like biped robot [10], [11], [12]. Instead, the basin of attraction of the limit-cycles related to the periodic walking has been enlarged in [13], also exploiting the energy pumping-and-damping passivity-based control. IDA-PBC has also been used as a tracking controller for fully actuated systems due to the possibility of assigning a desired pH structure to the closed-loop system [14], [15]. Consequently, the passivity of the closed-loop system is preserved, and damping can be injected into actuated coordinates. The methodology presented in [14] exploits the Cholesky factorization of the inertia matrix to retrieve a closed-loop structure with a novel, coordinates-free, kinetic energy. This is instrumental in designing a feedback control to assign a target error system that is uniformly globally exponentially stable (UGES). This stability property ensures strong robustness to the closed-loop system, motivated by total stability arguments [14]. The approach proposed in [15] obtains coordinate-free kinetic energy by using the square root factorization of the inertia

matrix. Both methodologies are limited to fully-actuated mechanical systems only.

This paper proposes a novel approach to realize a stable and periodic walking for a planar biped robot with one degree of underactuation, extending the methodology presented in [14]. The Cholesky factorization of the inertia matrix used therein is effectively exploited to separate actuated dynamics from unactuated ones. A feedback controller, composed of a tracking action inspired by [14] plus a compensation term cancelling the coupling elements between actuated and unactuated dynamics, is designed to track suitably defined joints trajectories. The resulting error system is the transverse dynamics that, thanks to the UGES property, converge exponentially fast to their zero dynamics manifold, with a convergence rate depending on the damping injection. Then, arguments from the theory of multiple Lyapunov functions for switched systems infer the hybrid invariance of the zero dynamics manifold. The motivation of such a control scheme is to preserve, as much as possible, the nonlinear dynamics of the system while increasing closed-loop robustness. The reasons behind choosing a control strategy based on [14] are twofold. First, like all IDA-PBC-based methodologies, the controller preserves the pH structure of the plant. Consequently, the closed-loop errors system is a passive pH system. Second, the Cholesky factorization used in [14] can be suitably exploited for underactuated systems, too, differently from the factorization method in [15]. Therefore, the main contributions of the work are(i) the proposed strategy confers robustness to the closed-loop system by assigning the desired error dynamics, which is a pH system preserving passivity; (ii) to the best of the authors' knowledge, the proposed approach is the first example of tracking controller based on the IDA-PBC applied to underactuated biped robots. In particular, the novel strategy extends the method in [14] to a class of underactuated hybrid systems.

II. Theoretical Background

A. Planar Bipeds as Underactuated Hybrid Systems

This work considers planar biped robots with symmetric and rigid legs and point feet. The gait is approximated with a sequence of single-support phases (only one foot in contact with the ground) followed by instantaneous double-support (both feet in contact with the ground). These assumptions are listed in [2] and [4, Chap. 3.2]. Single support phases correspond to the continuous dynamics characterizing the robot when no impact with the ground occurs. Instantaneous double-support phases represent the impulsive discrete event when feet strike the walking surface. Therefore, the underlying model is hybrid, describing the systems via a set of differential equations plus a set of difference equations

$$\begin{cases} \dot{x} = f(x) + \xi(x)u(x), & x \in X \backslash S, \\ x^+ = \Delta(x^-), & x^- \in S, \end{cases} \tag{1}$$

where $x \in X$ is the state, x^- and x^+ indicate the states just before and after an impact, respectively, $X \subseteq \mathbb{R}^{2n}$ is the admissibility domain of continuous dynamics, $f : X \to X$ is the C^1 vector field describing continuous dynamics, $\xi : X \to X$ is the C^1 vector field mapping the control input u to $f(\cdot)$, S is the switching surface, and $\Delta : S \to X$ is the C^1 reset map.

In literature, biped robots are usually described using the Lagrangian formalism, so the state of the system is described through a set of n generalized coordinates, $q \in \mathbb{R}^n$, and n generalized velocities, $\dot{q} \in \mathbb{R}^n$, such that $x = \begin{bmatrix} q^T & \dot{q}^T \end{bmatrix}^T \in \mathbb{R}^{2n}$. Due to the point-feet assumption, the biped is underactuated with one degree of underactuation [1]. A biped robot can be described by $n-1$ relative angles, representing body coordinates, plus an absolute angle representing the biped's orientation with respect to the z-axis of an inertial reference frame [4]. Body coordinates are related to the actuated joints, while the absolute angle is related to the unactuated one. Hence, the configuration of the biped can be expressed by $q = \begin{bmatrix} q_{a_1} & \cdots & q_{a_{n-1}} & q_u \end{bmatrix}^T \in \mathbb{R}^n$, where $q_{a_i} \in \mathbb{R}$, $i = 1, \ldots, n-1$, are the generalized coordinates corresponding to the actuated joints while $q_u \in \mathbb{R}$ is the coordinate related to the unactuated ankle. Besides, the absolute angle q_u is a cyclic variable of the kinetic energy [4]. Consequently, the inertia matrix does not depend on q_u and can be thus expressed as a function of the actuated coordinates only.

B. Virtual Constraints and Hybrid Zero Dynamics

A successful approach to realize stable periodic walking is to design a set of virtual constraints [2] in the form of output variables $y \in \mathbb{R}^m$ such that

$$y = h(q_a) - h_d(\theta(q)), \tag{2}$$

where $h(\cdot) \in \mathbb{R}^m$ is a function of the actuated coordinates only, while $h_d(\cdot) \in \mathbb{R}^m$ is the desired trajectory that the actuated coordinates have to track. This is parameterized in terms of $\theta(\cdot) \in \mathbb{R}$, a function of q that substitutes the time in the periodic orbit parameterization. Hence, it has to be strictly monotonic. The desired function $h_d(\cdot)$ is designed using Bézier polynomials to impose constraints regarding the feasibility of the gait (the fulfilment of constraints regarding friction cones, for instance), its periodicity, sought gait descriptors (step length and period), and energy efficiency [1]. The approaches based on HZD [2], [4], [5], [6] impose the set of virtual constraints (2) using an appropriate control law. The actuated variables track a given state-dependent trajectory described via $h_d(\cdot)$. Periodic walking arises when (2) are zeroed. The dynamics of the hybrid system (1) evolve on a lower-dimensional submanifold, and the stability of the periodic orbit can be studied therein. In other words, the stability of the periodic orbit of (1) is equivalent to the stability of the HZD's periodic orbit

$$\begin{cases} \dot{z} = f_Z(z) & z \in Z \backslash S \\ z^+ = \Delta_{S \cap Z}(z^-) & z^- \in S, \end{cases} \tag{3}$$

where $Z \subset X$ is the HZD submanifold, while $f_Z(\cdot)$ and $\Delta_{S \cap Z}(\cdot)$ are the restrictions of $f(\cdot)$ and $\Delta(\cdot)$ to it, respectively. As pointed out in the Introduction, this is true for planar bipeds if the dynamics associated with the output variables approach exponentially fast to the HZD submanifold.

C. Passivity-Based Approach

One of the objectives of the passivity-based tracking controller presented in this work is to preserve, as much as possible, the original nonlinear dynamics of the system. Among the control strategies based on HZD available in the literature, only the passivity-based approach introduced in [6] shares the same goal. For the sake of comparison, let briefly summarize the main aspects of the strategy shown in [6]. Let $M \in \mathbb{R}^{n\times n}$ be the symmetric, positive definite inertia matrix of the biped, $N = C(q,\dot{q})\dot{q} + g(q) \in \mathbb{R}^n$ be the drift vector with $C \in \mathbb{R}^{n\times n}$ the Coriolis-centrifugal effects matrix and $g \in \mathbb{R}^n$ the gravitational forces vector, $B = \begin{bmatrix} I_{(n-1)\times(n-1)} & 0 \end{bmatrix}^T \in \mathbb{R}^{n\times(n-1)}$ the input mapping matrix, and $u \in \mathbb{R}^{n-1}$ the control input. Therefore, the Lagrangian model describing the swing phase is $M(q_a)\ddot{q} + N(q,\dot{q}) = Bu$. Exploiting the natural partition between actuated and unactuated dynamics as in [6], this equation can be split as

$$\begin{cases} M_{aa}\ddot{q}_a + M_{au}\ddot{q}_u + N_a = u, \\ M_{ua}\ddot{q}_a + M_{uu}\ddot{q}_u + N_u = 0, \end{cases} \tag{4}$$

with $N_a = C_{aa}\dot{q}_a + C_{au}\dot{q}_u + g_a$ and $N_u = C_{ua}\dot{q}_a + C_{uu}\dot{q}_u + g_u$, that can be rewritten as

$$\begin{cases} \bar{M}(q_a)\ddot{q}_a + \bar{N}(q,\dot{q}) = u, \\ \ddot{q}_u = -M_{uu}^{-1}(M_{ua}\ddot{q}_a + N_u), \end{cases} \tag{5}$$

with $\bar{M}(q_a) = M_{aa} - M_{au}M_{uu}^{-1}M_{ua}$ and $\bar{N}(q,\dot{q}) = -M_{au}M_{uu}^{-1}N_u + N_a$. Starting from the above equation, [6] proposes the following control strategy

$$u = \bar{M}\ddot{h}_d - (K_p y + (L + K_d)\dot{y}) + \bar{N}, \tag{6}$$

where L is a combination of terms belonging to M and C, not reported here for space reasons, while $K_p, K_d \in \mathbb{R}^{(n-1)\times(n-1)}$ are positive definite gain matrices. $\bar{N}$ is designed to cancel part of the natural actuated dynamics (for further details see [6, Sec. III-B]). Therefore, this methodology requires the partial cancellation of the nonlinear dynamics of the plant.

D. The IDA-PBC Tracking Controller

The strategy presented in this work is rooted in the pH formalism and based on the tracking controller proposed in [14], which is now briefly introduced. Even if the methodology originally proposed in [14] was tailored for fully-actuated mechanical systems ($q \equiv q_a$ and $p \equiv p_a$), the subscript a (actuated) will be used in this section to stress the difference between the original methodology and the novel approach which is the main contribution of the paper.

Consider a fully-actuated mechanical system represented in the pH formalism as

$$\begin{bmatrix} \dot{q}_a \\ \dot{p}_{a_0} \end{bmatrix} = \begin{bmatrix} O_n & I_n \\ -I_n & O_n \end{bmatrix} \begin{bmatrix} \nabla_{q_a} H_0(q_a, p_{a_0}) \\ \nabla_{p_{a_0}} H_0(q_a, p_{a_0}) \end{bmatrix} + G u_a(q_a, p_{a_0}) \tag{7}$$

where $O_n \in \mathbb{R}^{n\times n}$ and $I_n \in \mathbb{R}^{n\times n}$ are the zero and the identity matrices of the proper dimensions, respectively, $G \in \mathbb{R}^{2n\times n}$ is the input mapping matrix, and $u_a \in \mathbb{R}^n$ is the control input. $q_a \in \mathbb{R}^n$ are the generalized coordinates and $p_{a_0} \in \mathbb{R}^n$ are the conjugated generalized momenta. The total (mechanical) energy of the system is described by the Hamiltonian $H(q_a, p_{a_0}) = \frac{1}{2} p_{a_0}^T M^{-1}(q_a) p_{a_0} + V(q_a)$, where $V \in \mathbb{R}$ is the potential energy. As preliminary step to apply the tracking controller proposed in [14], the following change of momenta $p_a = T^T(q_a) p_{a_0}$ is performed, where $T(q_a)$ is the lower-triangular Cholesky factor of $M^{-1}(q_a)$, such that $M^{-1}(q_a) = T(q_a)T^T(q_a)$. With this change of momenta, (7) becomes

$$\begin{bmatrix} \dot{q}_a \\ \dot{p}_a \end{bmatrix} = \begin{bmatrix} O_n & T(q_a) \\ -T^T(q_a) & S(q_a, p_a) \end{bmatrix} \begin{bmatrix} \nabla_{q_a} H(q_a, p_a) \\ \nabla_{p_a} H(q_a, p_a) \end{bmatrix} + G v_a(q_a, p_a), \tag{8}$$

with the Hamiltonian now being $H(q_a, p_a) = \frac{1}{2} p_a^T p_a + V(q_a)$, where the kinetic energy $K(p_a) = \frac{1}{2} p_a^T p_a$ does not depend anymore on q_a. The change of momenta introduces a novel skew-symmetric, gyroscopic forces matrix $S(q_a, p_a) = \sum_{i=1}^{n} [(p_a^T T^{-1} \nabla_{q_i} T)^T (T^T e_i)^T - (T^T e_i)(p_a^T T^{-1} \nabla_{q_i} T)] : \mathbb{R}^n \times \mathbb{R}^n \to \mathbb{R}^{n\times n}$ with e_i the $i-th$ euclidean basis vector of $\mathbb{R}^n$. The new control input is $v_a(q_a, p_a) = T^T(q_a) u_a(q_a, p_{a_0}) \in \mathbb{R}^n$. Let $q_d(t)$ be the reference trajectory for actuated coordinates and $p_d(t) = T^{-1}(q_a)\dot{q}_d$ be the corresponding reference momenta. Defined $\tilde{q} = q_a - q_d(t)$ and $\tilde{p} = p_a - p_d(t)$ as the trajectory and the related momenta tracking errors, respectively, the tracking controller presented in [14] is

$$\begin{aligned} v_a = & -\frac{d}{dt}(T^{-1}(q_a))R_1\tilde{q} + \dot{p}_d(t) - S(q_a, p_a)p_d(t) \\ & - T^T(q_a)[\tilde{q} - \nabla_{q_a} V(q_a)] + [S(q_a, p_a) - R_2]T^{-1}(q_a)R_1\tilde{q} \\ & - T^{-1}(q_a)R_1 T(q_a)\tilde{p} - R_2\tilde{p}, \end{aligned} \tag{9}$$

where R_1, $R_2 \in \mathbb{R}^{n\times n}$ are positive definite dissipation matrices. Defined

$$w_1 = \tilde{q}\ ,\ w_2 = T^{-1}(q_a)R_1\tilde{q} + \tilde{p}, \tag{10}$$

the closed-loop pH system (8) with v_a as in (9) is equal to

$$\dot{w} = \begin{bmatrix} -R_1 & T(q_a) \\ -T^T(q_a) & S(q_a, p_a) - R_2 \end{bmatrix} \nabla H_d(w), \tag{11}$$

where

$$H_d(w) = \frac{1}{2}|w_1|^2 + \frac{1}{2}|w_2|^2 \tag{12}$$

is the Hamiltonian in the error variables. In [14], it is shown that

$$\dot{H}_d(w) = -||w_1||_{R_1}^2 - ||w_2||_{R_2}^2 \leq -\delta H_d(w) \tag{13}$$

with $\delta = 2min\{\lambda_{min}(R_1), \lambda_{min}(R_2)\} > 0$, hence the equilibrium point of (11) is UGES implying that both $\tilde{q}$ and $\tilde{p}$ go to zero exponentially fast, with the rate of convergence that can be adjusted via R_1 and R_2. This is a fundamental property of (11), which will be usefully exploited in the next section to counteract the repulsive behavior of the reset map.

III. Main Contribution

After a suitable momenta transformation $p = T^T(q)p_0$, the continuous dynamics of a planar biped robot can be described, similarly to (8), as

$$\begin{bmatrix} \dot{q} \\ \dot{p} \end{bmatrix} = \begin{bmatrix} O_n & T(q_a) \\ -T^T(q_a) & S(q_a, p) \end{bmatrix} \begin{bmatrix} \nabla_q H(q,p) \\ \nabla_p H(q,p) \end{bmatrix} + G v(q,p), \tag{14}$$

with $H(q,p) = \frac{1}{2}p^T p + V(q)$. Differently from (8), equation (14) describes an underactuated mechanical system. In [14], the Cholesky factorization is used only for computational reasons. Instead, in this paper, the shape of $T(q_a)$ has a key role in designing the control law. The lower-triangular structure of $T(q_a)$ is such that $\dot{q}_a = T(q_a)p_a$: hence, $\dot{q}_a$ are not influenced by p_u. Moreover, since $T(q_a)$ is the Cholesky factor of $M^{-1}(q_a)$, it depends on q_a only. Consequently, $\dot{q}_a$ in (14) coincides with $\dot{q}_a$ in (8). This property is fundamental to extend (9) to underactuated planar bipeds. Before continuing, the main goal of the novel methodology is pointed out.

Problem Description: Consider an underactuated planar biped robot modeled by (1), with the swing dynamics described by (14). Once defined a set of virtual constraints (2) such that a stable periodic orbit is created in the HZD submanifold, find a passivity-based tracking controller based on (9) such that the transverse dynamics of the closed-loop system are equivalent to (11).

A. Fully Actuated/Unactuated Partition

To adapt (9) to track the desired trajectory for an underactuated planar biped, the natural partition between actuated and unactuated variables is exploited. Let $x = \begin{bmatrix} x_a^T & x_u^T \end{bmatrix}^T$ be the state of the system, with $x_a = \begin{bmatrix} q_a^T & p_a^T \end{bmatrix}^T \in \mathbb{R}^{2(n-1)}$ and $x_u = \begin{bmatrix} q_u & p_u \end{bmatrix}^T \in \mathbb{R}^2$ the actuated and the unactuated variables, respectively. Therefore, (14) can be rewritten as

$$\begin{bmatrix} \dot{x}_a \\ \dot{x}_u \end{bmatrix} = \begin{bmatrix} J_{aa} & J_{au} \\ -J_{au}^T & J_{uu} \end{bmatrix} \begin{bmatrix} \nabla_{x_a} H(x) \\ \nabla_{x_u} H(x) \end{bmatrix} + \begin{bmatrix} G_a \\ 0_2 \end{bmatrix} v(x), \tag{15}$$

where $J_{aa} = \begin{bmatrix} O_{n-1} & T_{aa}(q_a); -T_{aa}^T(q_a) & S_{aa}(q_a,p) \end{bmatrix} \in \mathbb{R}^{2(n-1)\times 2(n-1)}$ is a skew-symmetric matrix with $O_{n-1} \in \mathbb{R}^{(n-1)\times(n-1)}$ the zero matrix of proper dimensions, $T_{aa}(q_a) \in \mathbb{R}^{(n-1)\times(n-1)}$ the matrix extracted from the first $n-1$ rows by $n-1$ columns of $T(q_a)$, and $S_{aa}(q_a,p) \in \mathbb{R}^{(n-1)\times(n-1)}$ the same for $S(q,p)$. $J_{au} = \begin{bmatrix} 0_{n-1} & 0_{n-1}; -T_{au}(q_a) & S_{au}(q_a,p) \end{bmatrix} \in \mathbb{R}^{2(n-1)\times 2}$ is the matrix containing the coupling terms between actuated and unactuated dynamics, $T_{au} = \begin{bmatrix} t_{ua_1}(q_a) & \cdots & t_{ua_{n-1}}(q_a) \end{bmatrix}^T \in \mathbb{R}^{n-1}$ and $S_{au} = \begin{bmatrix} s_{a_1u}(q_a,p) & \cdots & s_{a_{n-1}u}(q_a,p) \end{bmatrix}^T \in \mathbb{R}^{n-1}$, while $0_{n-1} \in \mathbb{R}^{n-1}$ is zero vector of proper dimensions. Finally, $J_{uu} = \begin{bmatrix} 0 & t_{uu}(q_a); -t_{uu}(q_a) & 0 \end{bmatrix} \in \mathbb{R}^{2\times 2}$ is the square matrix accounting for the unactuated dynamics only. The new input mapping matrix is $G_a = \begin{bmatrix} 0_{(n-1)\times(n-1)} & I_{(n-1)\times(n-1)} \end{bmatrix}^T \in \mathbb{R}^{2(n-1)\times(n-1)}$.

B. IDA-PBC Tracking Controller for Underactuated Systems

The tracking controller (9) assigns the desired error dynamics (11), whose equilibrium is UGES, to the fully-actuated mechanical system (8). To yield the underactuated mechanical system (15) to an error system that is, as much as possible, similar to (11), the control law

$$v = v_c + v_t \tag{16}$$

is proposed. This control law differs from (9). In particular, the first term, $v_c \in \mathbb{R}^{n-1}$, is designed to transform the actuated dynamics in (15) such as to mimic (8); the second term, $v_t \in \mathbb{R}^{n-1}$, is the effective tracking contribution, inspired to (9). The actuated dynamics in (15) are $\dot{x}_a = J_{aa}\nabla_{x_a}H(x) + J_{au}\nabla_{x_u}H(x) + G_a v$, equivalent to

$$\dot{x}_a = \begin{cases} \dot{q}_a = O_{n-1}\nabla_{q_a}V(q) + T_{aa}p_a \\ \dot{p}_a = -T_{aa}^T\nabla_{q_a}V(q) + S_{aa}p_a \\ \qquad -T_{au}\nabla_{q_u}V(q) + S_{au}p_u + v_c + v_t. \end{cases} \tag{17}$$

The vector $\dot{q}_a$ in (17) already coincide with $\dot{q}_a$ in (8) thanks to the particular structure of T_{aa}, as previously outlined. Therefore, the specific role of v_c is to compensate for the terms due to the unactauted dynamics in $\dot{p}_a$. Designing v_c as

$$v_c = T_{au}\nabla_{q_u}V(q) - S_{au}p_u \tag{18}$$

and substituting it back in (17) yields

$$\dot{x}_a = \begin{cases} \dot{q}_a = T_{aa}p_a \\ \dot{p}_a = -T_{aa}^T\nabla_{q_a}V(q) + S_{aa}p_a + v_t, \end{cases} \tag{19}$$

which is very similar to (8). The only difference is the term $T_{aa}^T\nabla_{q_a}V(q)$ which, due to $V(q)$, is function of both the actuated and the unactuated coordinates, while $T^T\nabla_{q_a}V(q_a)$ in (8) is function of the actuated coordinates only. Once defined v_c as in (18), the resulting closed loop becomes

$$\begin{bmatrix} \dot{x}_a \\ \dot{x}_u \end{bmatrix} = \begin{bmatrix} J_{aa} & 0_{2(n-1)\times 2} \\ -J_{au}^T & J_{uu} \end{bmatrix} \begin{bmatrix} \nabla_{x_a} H(x) \\ \nabla_{x_u} H(x) \end{bmatrix} + \begin{bmatrix} G_a \\ 0_2 \end{bmatrix} v_t(x). \tag{20}$$

Since the forces $J_{au}\nabla_{x_u}H(x)$, not present in (8), were removed from (15), the actuated dynamics of (20) can be now treated similarly to (8). To impose (2) through v_t, the tracking errors defined in Section II-D are replaced with $\tilde{q} = q_a - q_d(\theta(q))$ and $\tilde{p} = p_a - T_{aa}^{-1}(q_a)\dot{q}_d$, where $q_a \equiv h(q_a)$ and $q_d(\theta(q)) \equiv h_d(\theta(q))$. The novel tracking controller becomes

$$\begin{aligned} v_t = &-\frac{d}{dt}(T_{aa}^{-1}(q_a))R_1\tilde{q} + \dot{p}_d - S_{aa}(q_a,p)p_d \\ &- T_{aa}^T(q_a)[\tilde{q} - \nabla_{q_a}V(q)] + [S_{aa}(q_a,p) - R_2]T_{aa}^{-1}(q_a)R_1\tilde{q} \\ &- T_{aa}^{-1}(q_a)R_1T_{aa}(q_a)\tilde{p} - R_2\tilde{p}, \end{aligned} \tag{21}$$

with $R_1, R_2 \in \mathbb{R}^{(n-1)\times(n-1)}$ positive definite matrices yielding to the closed loop

$$\dot{w} = \begin{bmatrix} -R_1 & T_{aa}(q_a) \\ -T_{aa}^T(q_a) & S_{aa}(q_a,p) - R_2 \end{bmatrix} \nabla H_d(w), \tag{22}$$

where w_1 is defined as in (10) and $w_2 = T_{aa}^{-1}(q_a)R_1\tilde{q} + \tilde{p}$, with $H_d(w)$ given by (12).

Remark I Equation (22) can be interpreted as the transverse dynamics of the planar biped robot. Hence, the UGES property of the zero equilibrium point of (22) implies that the transverse dynamics converge to their zero dynamics uniformly exponentially fast, i.e., that the zero dynamics manifold has been made UGES. Moreover, since (22) is a pH system, transverse dynamics are passive.

Remark II As shown in Section II.C, the control design in (6) drops $\bar{N}$ from the model. On the other hand, (18) cancels $J_{au}\nabla_{x_u}H(x)$, which couples actuated and unactuated dynamics. This reshapes the actuated dynamics as in (8). In this way, (21) can be used, leading to (22).

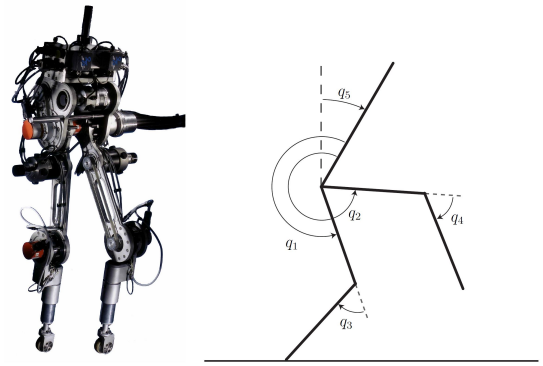

Fig. 1. RABBIT (left) and its physical idealization with coordinates system (right). The figure is taken from [5].

C. Stability Analysis

The stability analysis of the orbit can be performed using the Poincaré map of the system restricted to the HZD manifold [2], [5], [6]. To extend the stability of the orbit contained in the HZD manifold to the full-order system, the complete dynamics stability analysis is performed using the *conditional stability theorem for invariant sets* [16] and the *multiple Lyapunov functions theorem* [17]. Albeit the complete set of conditions is not reported here (see [6, Sec. IV]), they can be summarized with two main requirements: *i)* the Hamiltonian is decreasing during swing dynamics (i.e., $\dot{H}_d(w) \leq 0$); *ii)* the sequence of the Hamiltonian functions measured after each impact is decreasing. The first condition is strictly satisfied by (13). The second condition depends on the convergence rate of the transverse dynamics w_1 and w_2 to the HZD manifold. This is selected by tuning the dissipation matrices $R1$ and R_2, as discussed at the end of Section II.D.

IV. Case Studies

The proposed methodology has been applied in simulation to the model of a five-link bipedal robot inspired by RABBIT, a robotic test-bed developed to study dynamic walking [18], as done in [5] (see Fig. 1). The biped is made of the torso and two legs equipped with revolute knees. In the single support phase, the five-link biped can be described with a suitable set of coordinates $q \in \mathbb{R}^5$, where q_1 and q_2 are the femur angles (referenced to the torso), q_3 and q_4 are the knee angles, and q_5 is the absolute angle of the torso. Femur and knee joints are independently actuated while stance ankle is unactuated. The hybrid model of RABBIT can be described as in (1) with continuous dynamics (14) (after a suitable change of momenta) where M and V are defined in [4].

For this specific test bed, $v_c = T_{au}\nabla_{q_5}V(q) - S_{au}p_5 \in \mathbb{R}^4$ with T_{au}, $S_{au} \in \mathbb{R}^4$. The tracking controller (21) has been designed with T_{aa}, S_{aa}, $R_1 = 200I_4$, and $R_2 = 200I_4 \in \mathbb{R}^{4\times4}$. Numerical simulations are performed on a standard PC in the MATLAB environment. The code for generating the dynamic model of RABBIT is taken from [19]. It has been numerically simulated through the *ODE*45 routine of MATLAB with the event detection option active to evaluate the foot-ground hit. The designed controller is implemented at a discrete-time step of 1 ms. In the literature, a step is defined as two consecutive strikes between feet and ground [10], [20]. The gait is described in terms of two parameters: the space covered by each step (the *step length*, $S > 0$) and its duration (the *step period*, $T > 0$). The target values are $T = 0.5$ s and $S = 0.4$ m, respectively. Such values are imposed through a 4×1 vector $h_d(\theta)$ of 6th degree Bézier polynomials parameterizing the desired periodic trajectory. This trajectory has been computed solving an offline optimization problem [2]. As in [2], [5], [6], θ has been selected as the angle between the vertical and the line connecting the stance foot to the hip. In the following, two case studies have been analyzed. In the first one, the performance of the presented controller is evaluated in nominal conditions, i.e., without parametric uncertainties affecting the model. In the second one, the claimed robustness of the novel methodology is assessed, i.e., it is tested in the presence of parametric uncertainties. Moreover, a comparison with the passivity-based controller proposed in [6] is performed. In both the case studies, initial conditions are picked outside the periodic orbit to show the exponential convergence of the output to zero. The overall gait considered is made of twenty steps.

In Case Study I, the performance of the proposed methodology is evaluated without parametric uncertainties on the dynamic model with parameters taken from [4]. Figure 2 depicts the limit cycles obtained corresponding to one actuated variable (q_1) and the unactuated one (q_5). Both cycles (blue lines) converge to the target ones (dotted red lines) corresponding to the desired gait associated with the values assumed by T and S, shown in Fig. 3. The time evolution of the H_d and the tracking errors $\tilde{q}$ and $\tilde{p}$ are shown in Fig. 4, Fig. 5, and Fig. 6, respectively, for the first four steps (the remaining sixteen steps have not been shown not to compromise the readability of the plots). Specifically, these figures point out the stability of the full-order system since H_d, $\tilde{q}$, and $\tilde{p}$ convergence exponentially fast to zero during the swing phase, and the sequence of values assumed by H_d at every impact is decreasing (Fig. 4 (b)).

In Case Study II, the proposed controller is tested against the presence of parametric uncertainties. The dynamic model parameters in the controller are affected by uncertainties in the range $10\% - 40\%$ of the nominal values. The proposed methodology, designed with the same gains as in Case Study I, is compared with the passivity-based controller of [6]. This has been designed using a set of gains exhibiting performance similar to those achieved deploying the novel controller in nominal conditions. In the simulations carried out with the 30% of uncertainty, both controllers show a stable behaviour of the closed-loop system. For the 40% of uncertainty, Fig. 7 shows that the proposed methodology does not compromise the system's stability. Indeed, H_d keeps decreasing during both swing phases and impact events. The same parametric uncertainties lead the closed-loop system to instability when controlled with the approach of [6], as evident from Fig. 8 (b) where the sequence of Lyapunov functions $V = \frac{1}{2}(\dot{y}^T\bar{M}\dot{y}) + \frac{1}{2}(y^T K_p y)$ [6] evaluated at each impact is not decreasing.

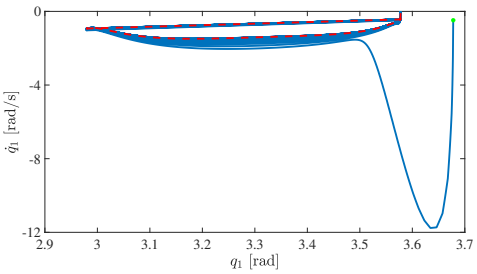

(a) Limit cycle of q_1.

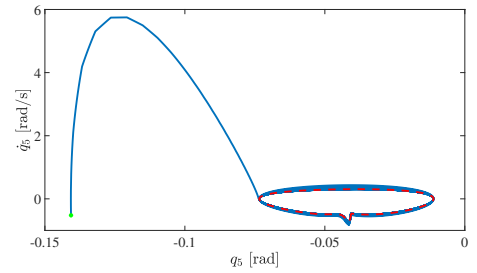

(b) Limit cycle of q_5.

Fig. 2. Case Study I, limit cycles of (a) q_1 and (b) q_5. Green dots: initial conditions. Blue lines: evolution of each limit cycle. Red lines: target cycles.

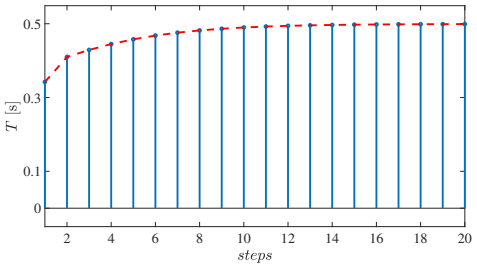

(a) Time history of T.

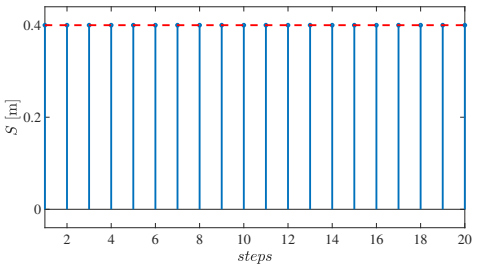

(b) Time history of S.

Fig. 3. Case Study I, step period T and step length S. Blue bars: the step-by-step evolution of (a) T and (b) S. The red lines show that T and S converge to their target values 0.5 s and 0.4 m, respectively.

V. Conlcusions and Future Work

This paper proposed a tracking controller based on the methodology presented in [14] with HZD for underactuated planar biped robots. The novel approach was shown to represent a valid alternative to existing control strategies to stabilize periodic walking. In particular, numerical simulations on a five-link walker validated the approach showing that the novel control strategy is robust even with strong parametric uncertainty. Future works will apply the presented methodology to a biped robot with more degrees of underactuation. In particular, the work will be extended to those bipeds that are not constrained to move in the sagittal plane only, also with compliant joints.

References

[1] J. W. Grizzle, C. Chevallereau, R. W. Sinnet, and A. D. Ames, "Models, feedback control, and open problems of 3d bipedal robot walking," *Automatica*, vol. 50, no. 8, pp. 1955–1988, 2014.

[2] E. R. Westervelt, J. W. Grizzle, and D. E. Koditschek, "Hybrid zero dynamics of planar biped walkers," *IEEE Trans. Automat. Control*, vol. 48, no. 1, pp. 42–56, 2003.

[3] A. Isidori, *Nonlinear Control Systems (3rd ed.)*. Berlin: Springer-Verlag, 1995.

[4] E. R. Westervelt, J. W. Grizzle, C. Chevallereau, J. H. Choi, and B. Morris, *Feedback Control of Dynamic Bipedal Robot Locomotion*. London, UK: Taylor & Francis/CRC Press, 2007.

[5] A. D. Ames, K. Galloway, K. Sreenath, and J. W. Grizzle, "Rapidly Exponentially Stabilizing Control Lyapunov Functions and Hybrid Zero Dynamics," *IEEE Trans. Automat. Control*, vol. 59, no. 4, pp. 876–891, 2014.

[6] H. Sadeghian, C. Ott, G. Garofalo, and G. Cheng, "Passivity-based control of underactuated biped robots within hybrid zero dynamics approach," in *2017 IEEE Int. Conf. Robot. Autom.*, Singapore, 2017, pp. 4096–4101.

[7] R. Ortega, A. Van Der Schaft, I. Mareels, and B. Maschke, "Putting energy back into control," *IEEE Control Syst. Mag.*, pp. 18–33, 2001.

[8] R. Ortega, A. Van Der Schaft, B. Maschke, and G. Escobar, "Interconnection and damping assignment passivity-based control of port-controlled Hamiltonian systems," *Automatica*, vol. 38, no. 4, pp. 585–596, 2002.

[9] R. Ortega, M. Spong, F. Gómez-Estern, and G. Blankenstein, "Stabilization of a class of underactuated mechanical systems via interconnection and damping assignment," *IEEE Trans. Automat. Control*, vol. 47, no. 8, pp. 1218–1233, 2002.

[10] V. De-León-Gómez, V. Santibanéz, and J. Sandoval, "Interconnection and damping assignment passivity-based control for a compass-like biped robot," *Int. J. Adv. Robot. Syst.*, vol. 14, no. 4, 2017.

[11] P. Arpenti, F. Ruggiero, and V. Lippiello, "Interconnection and damping assignment passivity-based control for gait generation in underactuated compass-like robots," in *2020 IEEE Int. Conf. Robot. Autom.*, 2020, pp. 9802–9808.

[12] P. Arpenti, F. Ruggiero, and V. Lippiello, "A constructive methodology for the ida-pbc of underactuated 2-dof mechanical systems with explicit solution of pdes," *Int. J. Control Autom. Syst.*, vol. 20, no. 2, pp. 283–297, 2022.

[13] P. Arpenti, A. Donaire, F. Ruggiero, and V. Lippiello, "Energy pumping-and-damping for gait robustification of underactuated planar biped robots within the hybrid zero dynamics framework," in *2020 IEEE-RAS Int. Conf. Humanoid Robots*, 2021, pp. 415–421.

[14] J. G. Romero, R. Ortega, and I. Sarras, "A globally exponentially stable tracking controller for mechanical systems using position feedback," *IEEE Trans. Automat. Control*, vol. 60, no. 3, pp. 818–823, 2015.

[15] J. Ferguson, A. Donaire, and R. H. Hiddelton, "Kinetic-Potential Energy Shaping for Mechanical Systems With Applications to Tracking," *IEEE Contr. Syst. Lett.*, vol. 3, no. 4, pp. 960–965, 2019.

[16] G. Garofalo, C. Ott, and A. Albu-Schäffer, "Orbital stabilization of mechanical systems through semidefinite lyapunov functions," in *2013 Am. Control Conf.*, 2013, pp. 5715–5721.

[17] M. Branicky, "Multiple lyapunov functions and other analysis tools for switched and hybrid systems," *IEEE Trans. Automat. Control*, vol. 43, no. 4, pp. 475–482, 1998.

[18] E. R. Westervelt, G. Buche, and J. W. Grizzle, "Experimental validation of a framework for the design of controllers that induce stable walking in planar bipeds," *Int. J. Robot. Res.*, vol. 23, no. 6, pp. 559–582, 2004.

[19] E. R. Westervelt, J. W. Grizzle, C. Chevallereau, J. H. Choi, and B. Morris. (2007) Feedback Control of Dynamic Bipedal Robot Locomotion. [Online]. Available: http://web.eecs.umich.edu/ grizzle/biped˙book˙web/

[20] J. Holm and M. W. Spong, "Kinetic energy shaping for gait regulation of underactuated bipeds," in *IEEE Int. Conf. Control Applications*, San Antonio, Texas, USA, 2008, pp. 1232–1238.

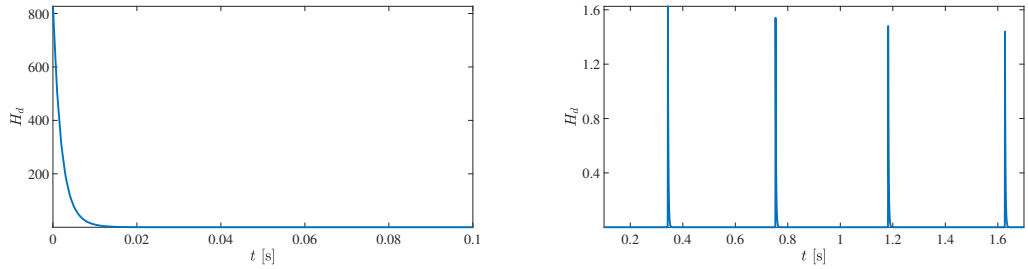

(a) H_d before the first step. (b) H_d at the first four steps.

Fig. 4. Case Study I, evolution of H_d. (a) Control law (16) drives H_d exponentially fast to zero. (b) H_d decreases at every impact.

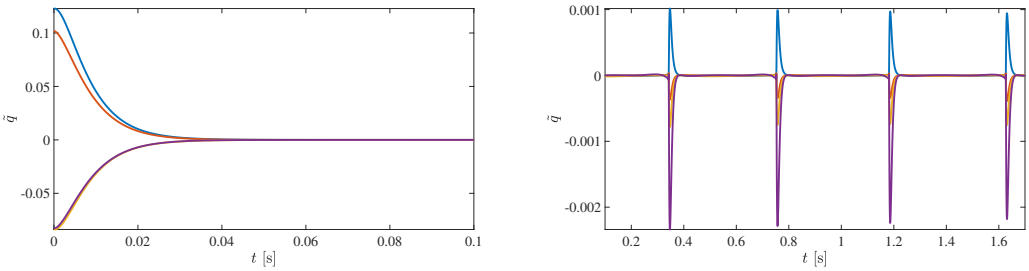

(a) $\tilde{q}$ before the first step. (b) $\tilde{q}$ at the first four steps.

Fig. 5. Case Study I, evolution of $\tilde{q}$. (a) Control law (16) drives $\tilde{q}$ exponentially fast to zero. (b) $\tilde{q}$ decreases at every impact.

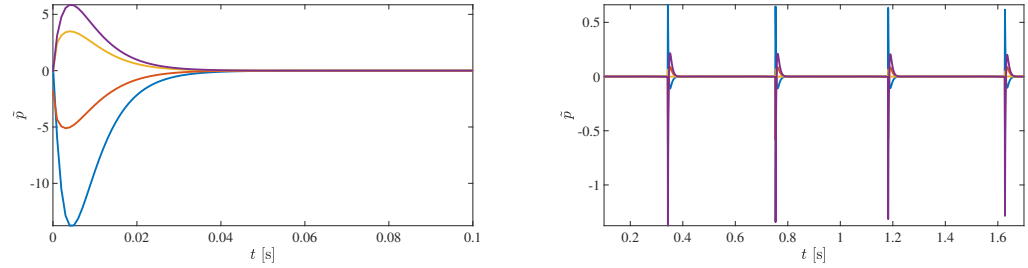

(a) $\tilde{p}$ before the first step. (b) $\tilde{p}$ at the first four steps.

Fig. 6. Case Study I, evolution of $\tilde{p}$. (a) Control law (16) drives $\tilde{p}$ exponentially fast to zero. (b) $\tilde{p}$ decreases at every impact.

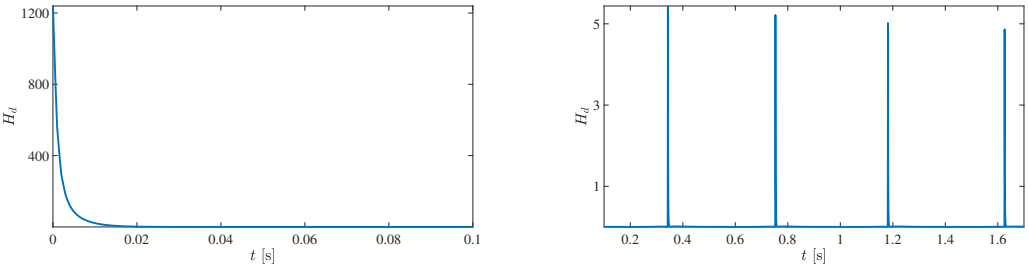

(a) H_d before the first step. (b) H_d at the first four steps.

Fig. 7. Case Study II, H_d evolution. (a) Control law (16) drives H_d exponentially fast to zero with 40% of uncertainty. (b) H_d decreases at every impact.

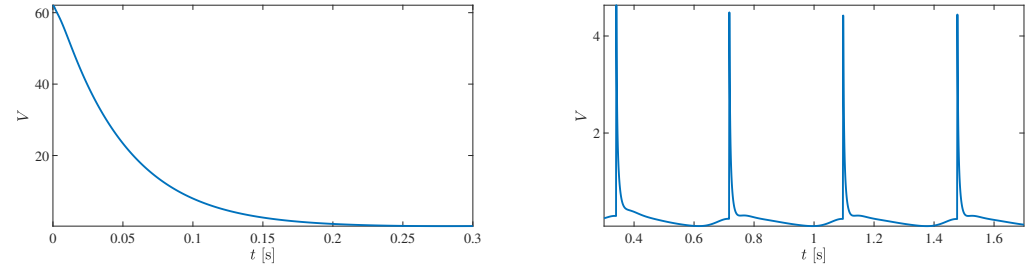

(a) V before the first step. (b) V at the first four steps.

Fig. 8. Case Study II, V evolution. (a) Controller (6) in [6] drives V exponentially to zero with 40% of uncertainty but V increases at the 4ˆth impact (b).